IEEE Access
Multidisciplinary | Rapid Review | Open Access Journal

Received 12 September 2023, accepted 28 September 2023, date of publication 2 October 2023, date of current version 9 October 2023.

Digital Object Identifier 10.1109/ACCESS.2023.3321219

APPLIED RESEARCH

Toward Smarter Grids: Experimental Investigation of an "All-Optical" Electrical Sensor Under Laboratory Conditions

KHALED OSMANI, MARC FLORIAN MEYER, FLORIAN GRUMM, AND DETLEF SCHULZ, (Senior Member, IEEE)
Department of Electrical Engineering, Helmut Schmidt University, 22043 Hamburg, Germany

Corresponding author: Khaled Osmani (alosmank@hsu-hh.de)

This work was supported by dtec.bw—Digitalization and Technology Research Center of the Bundeswehr through the Project "Digitalisierte, rechtssichere und emissionsarme flugmobile Inspektion und Netzdatenerfassung mit automatisierten Drohnen," engl. "Digitalised, legally safe and low-emission airborne inspection and grid data acquisition using automated drones" (DNeD).

ABSTRACT Smart grids yield in an efficient energy distribution, driven by advanced grid management and diverse technologies' integration. For instance, the remote monitoring of transmission lines, facilitates the development process of conventional electrical networks into smart grids. One form of such remote monitoring applications can be actuated by means of a drone, which carries an embedded intelligent sensor. These drone-based applications referred to as Unmanned Aerial Systems (UAS), thus allow an instantaneous surveillance of the actual status of transmission lines, remotely. Accordingly, this paper presents an experimental setup of an "all-optical" electrical sensor, confronted with different forced voltage/current (V/I) levels, in order to test its feasibility for future applications in drone-controlled, electric grid monitoring processes. After analyzing different measurements' outputs, and comparing them with reference values outputted by reference V/I sensors, the resulting deviated errors are tabulated and justified. Furthermore, the exploration of the studied sensor's pros and cons, and by taking into consideration the space/weight restrictions that a drone-based application obtrudes, related future work is suggested.

INDEX TERMS Electrical monitoring, non-invasive sensor, optical data, remote measurements, smart grids, transmission lines, unmanned aerial systems (UAS).

NOMENCLATURE

Abbreviations

$LiNbO_3$	Lithium niobate.
CT	Current Transformer.
DNeD	Digitalisierte, rechtssichere und emissionsarme flugmobile Inspektion und Netzdatenerfassung mit automatisierten Drohnen.
ESS	Energy Storage Systems.
IoT	Internet of Things.
LEA	Low Energy Analog.
PV	PhotoVoltaic.
TL	Transmission Line.
UAS	Unmanned Aerial System.
VT	Voltage Transformer.

Units

A	Amperes.
kVA	Kilo Volt Ampere (Complex power).
kWh	Kilo Watt Hour (energy).
V	Volts.

I. INTRODUCTION

In response with the growing energy demands (e.g., load demands of private, residential, and industrial sectors), evolved is an urge to add a certain "intelligence" onto conventional electrical grids. This needed intelligence becomes

The associate editor coordinating the review of this manuscript and approving it for publication was Diego Bellan.

compulsory, especially when taking into consideration the environmental concerns (i.e., to suppress the excessive burning of fossil fuels, mitigate the greenhouse gases emissions, and to protect the climate) [1]. Therefore, the evolution of smart grids is skyrocketing as a counter reaction to the increased energy demands, and to optimize the utilization of different resources. Such newer grids play a vital role in rending the electrical network more reliable, achieving better energy efficiency, and empowering consumers with a higher control over their energy consumption. The stated ''intelligence'' can be added over the traditional electric grids, through a digitalization process, thus revolutionizing the energy sector [2]. In other terms, the traditional power grids are upgraded to more intelligent and interconnected systems by means of the integration of advanced communication and information technologies. This integration would allow a real-time monitoring, thus consequently, an improved grid's flexibility and reliability. With that being said, electric grids are being modernized through digitalization, thus unleashing from the old analog systems barriers such as decreased reliability, reduced communication, and static efficiency [3]. For instance, a digitalized electric grid allows an optimized energy distribution, better load management, predictive fault detection, thus reducing probabilistic downtimes while improving the overall grid's performance. Additionally, data analytics and machine learning algorithms can be added over the ''digitalized'' grid as well. This in turns would enable the grid's operators thus to have in advanced general information over the grid's status, as well as predicting the demand patterns while proactively addressing different potential issues (e.g., grid's overloading) [4].

When compared to conventional analog grids, the digitalized electrical grids offer significant advantages, mainly the remote monitoring/controlling feature. This feature allows the grid operators to access real-time data on energy consumption, load patterns, and status of equipment from different nodes inside the grid. It also yields eventually to a swift detection and resolution of any form of malfunctioning, thus reducing the network's downtime while improving its operational efficiency [5]. The grid's settings as well as the load balancing can be hence remotely adjusted, therefore optimizing the energy distribution what results in turn in a higher grid's reliability. The stated real-time monitoring and analytics features offered by smart grids, contribute significantly towards better energy production efficiency, by enabling a deeper understanding of the energy consumption patterns as well as the demand fluctuations [6]. Accordingly, such insight gives a better advantage for more precise load balancing and optimized energy generation, what in turns yield to a reduced grid's power losses (i.e., wastage). Successively, when the transmission and distribution losses are minimized, the demand-side management is better promoted, yielding also to maximizing the energy production efficiency [7]. In terms of cleaner and carbonless electrical power production, smart grids also possess a good potential, driven mainly by facilitating their integration with renewable energy provisions, such as solar PhotoVoltaic (PV) and wind-based power resources, thus enabling a substantial reduction in greenhouse gas emissions [8]. With the added intelligence over the traditional electric grids, the latent intelligently cooperate with the intermittent nature of renewable energy supplies. For example, smart grids incorporate a flexible and automated connection with Energy Storage Systems (ESS), such as batteries banks [9].

With the advanced monitoring capabilities hence offered by the smart grids, the ''decision-making'' cases related to electrical load optimization can be conducted more accurately. On the first hand, consumers can be directed accordingly to shift their energy usage for example to times under which the supply from the renewables is more abundant (e.g., peak hours of solar irradiance). With the digitalized feature of smart grids on the other hand, the implementation of advanced sensors, analytics and forecasting algorithms, can maximize the contribution from the renewable energy sources with respect to the overall energy mix. With such a reliable integration between renewable supplies and smart grids, the overall energy production can be decentralized. This would hence allow a portion of the grid's power to be generated from the local consumers' excess power production from renewable energy. Consequently, the dependency on fossil fuels would be reduced, paving a way for a greener future of energy. With the advantages presented by the smart grids and the advanced grid technologies, an international strong emphasis on encouraging the research and development in such fields (i.e., grid resilience, cyber security, advanced energy storage, etc.) is emerged by governments and research institutions. Accordingly, due to the international collaboration and expertise exchange, the advancements in the smart grids' technologies are rapidly expanding, hence better accelerating towards cleaner production [10]. For the case of Europe for example, the future vision of smarter electrical grids is focused on the creation of resilient, sustainable, and interconnected energy systems, with a highly reliable grid's infrastructure, that allows a seamless integration with electric vehicles and charging stations. Other than the stated smart grids' advantages, they can be expanded and coupled with cloud applications and Internet of Things (IoT) facilities [11].

On the first hand, cloud-based platforms enable the scalability of the large produced data between many smart grids, allowing thus an instantaneous monitoring of different grids, with a remote-control ability. Within each smart grid, on the other hand, the IoT establishes connectivity and communication routes between various devices and sensors. In addition to facilitating more efficient data exchange, such IoT driven communication yields in a more accurate predictive maintenance scheme and more optimized demand response [12]. From a realistic approach, the stated smart grids' advancements with their numerous advantages are almost only theoretically feasible. In other terms, the transformation process of conventional electric grids into smart

ones, is not a straight forward approach, rather a challenging task that can be prohibited due to many obstacles. On the first hand, the conventional electric grids are steeped in tradition, reflecting the outcomes of an outdated technology [13]. Built upon aging infrastructure, such conventional grids struggle to meet the evolving energy demands. Beside than being characterized by their inherent unreliability, where they cannot be addressed remotely, through network communications for example, other vulnerabilities lie in complex factors such as:

- Aging equipment
- Limited capacity for load balancing
- Susceptibility to weather related disruptions.

Aside to their stated intrinsic unreliability, conventional electrical grids in different regions of the world are often pushed to their extreme capacities. They hence face significant limitations in terms of expandability for integration with newer technologies that aim to add ''intelligence'' on them. Different obstacles, such as limited physical space, high costs of installation, and subsequent maintenance costs, pose a great challenge in front of any external technological implementation on conventional grids. Following the same perspective regarding the stubborn nature of conventional electrical grids, that hardly allows for any extra circuitry to be added onto, they are inherently prone to different types of faults. Additionally, they are susceptible to operational issues that compromise their applicability with additive external circuitry (e.g., advanced sensors, smart switchgear, etc.) [14]. Also, the initial reliance of conventional grids on legacy systems, such as Current Transformers (CT) and Voltage Transformers (VT) for measuring applications, in turns poses additional challenges in front of any advanced metering infrastructure's future implementation. The previously stated digitalization process of conventional grids, is as hard as adding intelligence over them. From one side, the age and diversity of equipment in old electrical grids makes it harder to establish a common protocol that can be referenced to as standard between different devices (i.e., CT, VT, etc.). On the other hand, the limited availability of historical data, in addition to the absence of comprehensive asset management systems, complicate the equipment's status prediction and the overall performance degradation assessment. For this reason, machine-based models for example, become harder to integrate effectively with conventional grids, due to the existing information gaps. The stated technical challenges and engineering complexities, imposed in front of the transformation of conventional electrical grids (i.e., of old nature) into smarter grids (i.e., achieving better and more reliable energy efficiency) are thoroughly researched in order to find an optimum solution. Modern research for smart grids transformation is mainly concerned with the following key topics:

- Smart energy (kWh) meters [15]
- Distribution automation [16]
- Microgrids [17]

The smart kWh meters provide real-time data on energy consumption, allowing thus a better monitoring capability for both users and utility companies. Such meters would yield in better informing the energy customers about their consumption patterns, resulting thus with potential energy cost savings. Aside than the instantaneous monitoring capability offered by such meters, they also enable a two-way communication between power consumers and generation facilities, enabling hence better load balancing with the grid. On the other hand, one potential drawback of smart kWh meters is their high initial cost of installation, as compared to traditional meters. Extra infrastructure is also needed to support smart meters (e.g., communication networks, data management systems). Since smart meters transmit sensitive information about the consumers' energy usage, additional concerns should be taken into consideration regarding the data privacy issue and cybersecurity. Distribution automation from another side, adds a certain ''intelligence'' over traditional electrical grids, mainly by automating various processes such as fault detection and service restoration, thus reducing the downtimes associated with power outage. However, and as it is the case with the smart kWh meters, the distribution automation compels a high upfront cost for installing a certain infrastructure, including sensors, control systems, communication protocols, and a skilled workforce (i.e., experienced labors).

By providing localized power generation and distribution facilities, microgrids can as well enhance a conventional electrical grid's resiliency. Microgrids possess also the ability to continuously supply electrical power to critical loads for example, during power outage or general system failures. With the application of microgrids, the downtimes are hence reduced, along with their negative impact over essential services (e.g., banks, hospitals, etc.). With the localized power generation, and the decreased dependencies on the centralized power plants, the transmission losses consecutively are decreased, achieving hence a better energy efficiency. Despite the fact that microgrids might succeed to add a certain intelligence on conventional grids, they impose on the other hand, the need of a complex infrastructure which requires the installation of extra circuitry for control and monitoring equipment. Additionally, microgrids can be subject to further technical challenges confronted especially under the coordination and management of multiple interconnected microgrids.

Although that the proposed solution methods (i.e., smart meters, microgrids, etc.) achieve somehow a success in transforming the conventional electric grids into smarter grids, but as can be seen from the stated small survey, that each method presents its own disadvantages. It can be stated that all of these techniques share in common the need of expensive additive costs in order to be realized. For that purpose, the usage of drone-based applications, such as the one in the ''Digitalisierte, rechtssichere und emissionsarme flugmobile Inspektion und Netzdatenerfassung mit automatisierten Drohnen (DNeD)'' project [18], can remotely add the needed ''intelligence'' over the existing electrical grids, while requiring a less financial burden as compared to other methodologies. From a first point of view, the drone-based

applications require no extra circuitry to be installed onto the conventional grid. A drone can temporarily acquire data from over the transmission line for example, in a contactless manner. A smart sensor can be hence integrated, where it can remotely sense and measure different electrical attributes (mainly voltage and current). Eventually, this combinatorial scheme would better give an overall information about the grid's status. Using such a methodology requires less data concerns as well as complex monitoring equipment as was the case in the previous reviewed research. A drone-based remote grid sensing method is centrally based on the designed sensor that is to be integrated with it. Assumed to be of a non-invasive nature, the sensor must present accurate electrical measurements, while not imposing any extra weight on the drone. For that purpose, this paper aims to investigate the behavior of an all-optical electrical sensor from Micatu [19], referred to as GridView RG235 which represents a modular voltage and current sensor [20]. Under laboratory conditions, the GridView RG235 has its feasibility tested for future employment in the DNeD project.

The remainder of this paper consists as follows: Section II presents an overview of the RG235 working methodology and principles of operation. Section III consists of the actual experimental setup of the sensor under laboratory conditions for voltage and current measurements, indicating in details the procedures of different circuits realizations. In Section IV, presented are the results with their relative observations and analysis, additionally to the recommended future work for the destined sensor to be employed in the DNeD. Finally in Section V, conclusions are derived.

II. THE RG235 WORKING METHODOLOGY

For drone-based electric Transmission Line (TL) monitoring processes, generally controlled by means of Unmanned Aerial Systems (UAS), the contactless voltage/current sensors are the only feasible option for such applications. The contactless (i.e., non-invasive) sensors can be freely dropped-off/picked-up by the drone without any need to physically interact with the TL's bare conductor. In other words, it is not possible for an intrusive voltage/current sensor to be incorporated with a UAS-controlled drone-based TL monitoring application. Accordingly, and among different types of contactless electrical sensors (i.e., hall-effect, Rogowski coil, magnetic tunnel junction, constant capacitive coupling, etc. [21]), the optical-based sensors are the most recommended for UAS-controlled TL monitoring processes, due to the following reasons:

a) Optical sensors would not saturate (unlike magneto-based contactless sensors), since they possess no magnetic core
b) Provide more accurate sensing resolution, and are better immune to external interfering noise
c) Under faulty conditions, optical sensors better fail-safe, with less risks as compared to other types of contactless sensors

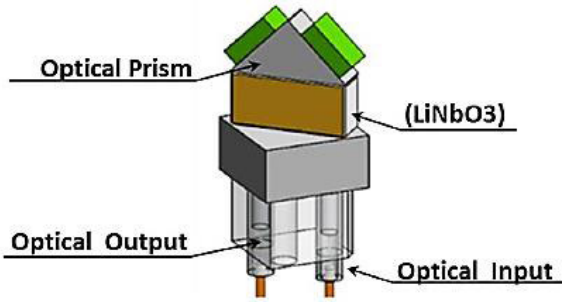

FIGURE 1. Pockels electro-optical based voltage sensor [22].

Since it is theoretically possible to have an all-optical sensor that combines the ability to measure both voltage and current quantities, hence such a sensor would impose less space requirements and would better fit in a drone. For each of the mentioned reasons, in addition to a remote ability for voltage/current measurements, an all-optical electrical sensor is hence chosen to be tested and experimented with a future target to actually employ it into a drone, for a remote TL monitoring as in [18]. Therefore, an "intelligence" can be relatively added to an electric grid. Consequently, the Micatu GridView – RG235 all-optical sensor is chosen to have its outcomes investigated, and furtherly studied for any possible future incorporation with a drone for a remote TL monitoring application. The suggested RG235 sensor, in addition to presenting accurate voltage data for up to 35 kV, it also can simultaneously measure current, frequency (50 to 60 Hz), and harmonics (up to the 11^{th} harmonic). Moreover, the RG235 can be "online" installed, requiring hence no need for any power shutdown, thus provoking no electrical power outage [20].

A. PRINCIPLE OF VOLTAGE MEASUREMENT

By emphasizing on the Pockels' effect law, as depicted in (1), which states that a medium's refractive index is proportionally modified with respect to the applied electric field's strength, the core of the voltage sensor in the RG235 shown in Figure 1 operates accordingly.

$$V(t,T) = \frac{V_\pi(T)}{\pi}\sqrt{\frac{P_{AC}(t,T)}{P_{DC}}} - C(T) \tag{1}$$

Such that V_π represents the half-wave voltage of the transverse modulator, P_{AC} the optical AC modulated power on the photodiode with P_{DC} its Direct Current (DC) component, and $C(T)$ the calibration factor [22].

The optical prism shown in Figure 1 translates the phase retardation induced in the polarized light, after passing through the non-centrosymmetric material (i.e., Lithium niobate ($LiNbO_3$)) into an equivalent voltage. The stated phase retardation is a linear function of the applied voltage (in parallel to the $LiNbO_3$ optical axis of the applied incident light) [22]. Therefore, when the prism of Figure 1 is placed perpendicularly to the electric field (produced by the high

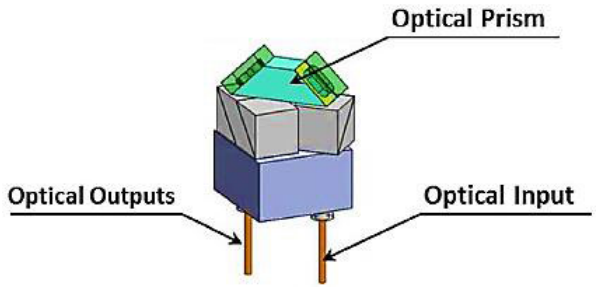

FIGURE 2. Faraday's electro-optical based current sensor [24].

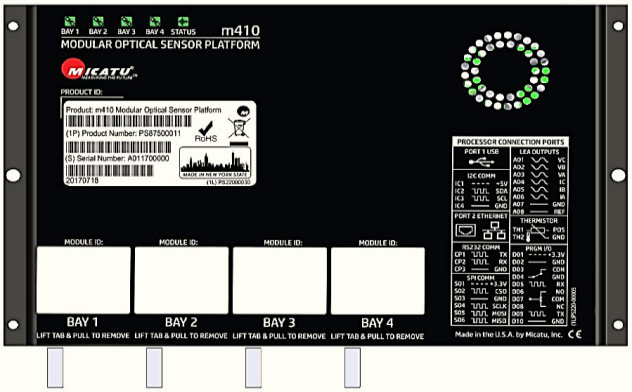

FIGURE 3. The M410B optical modulator [25].

voltage pickoff rod, between the line potential and the ground, inside the Cycloaliphatic Epoxy body of the RG235), having the dielectrics (of the surrounding insulator body) meeting the voltage class rating of the measurement application: the applied voltage's ''image'' can be constructed and acknowledged. The following workflow (referenced with Figure 1 components) states how the RG235 acquires the information about the voltage to be measured [22]:

1. The retro-prism material (optical prism in Figure 1) is coupled to the crystal material ($LiNbO_3$) and is configured to receive the light propagated through $LiNbO_3$, then reflect the propagated light beam back into $LiNbO_3$
2. The optical output is positioned to receive the light directed by the optical prism assembly back through the crystal material
3. The optical output is then coupled to the optical input in order to provide it with the polarized light resulting from the crystal material (according to the Pockels' effect)
4. The optical input can be any type of a laser diode, producing a spatially/partially coherent light beam
5. The optical output receives the light beams when they get reflected back through the crystal material by the optical prism
6. The optical phase of the produced light beams (i.e., representing the source of information for the applied voltage) is hence measured by the optical output

B. PRINCIPLE OF CURRENT MEASUREMENT

In addition to the previously stated voltage measuring mechanism held by the RG235, the latent can simultaneously sense current by means of an optical Faraday magneto-optical based sensor, as presented in Figure 2, having its mathematical formulation depicted in (2) [23].

$$\varphi = \mu \cdot V \cdot \int Hdl \tag{2}$$

Such that μ ,V represent the magneto-optical material's relative permeability and Verdet constant respectively, and H the magnetic field intensity generated by the measured current [23]. According to (2), it can be stated that an applied current can be indirectly calculated after knowing its resulting magnetic field, which in turn acts proportionally on the degree of the light's polarization rotation.

The prism shown in Figure 2 translates the polarization rotation produced in the polarized light, due after that the magnetic-optical material is exposed to a magnetic field (i.e., resulting by the current flow), to an equivalent current ''image''. In other terms, the amount of polarization rotation is directly proportional to the resulting magnetic field which is induced by the current flow. Accordingly, when the prism of Figure 2 is placed between the magnetic field flux, by taking into consideration that its optical path must be as well placed in parallel to the active magnetic field, having also its top surrounded by a magnetic flux concentrator, the initially applied current's ''image'' can be constructed. The current is hence acknowledged according to the following work flow [24]:

1. The optical input transmits the beam of the polarized electromagnetic radiation to the polarized light input of the optical prism
2. The optical output transmits then the beam of the polarized electromagnetic radiation from the light output of the optical prism, to an external light detector
3. For both steps in 1. and in 2., a magnetic concentrator is supposed to be in a closed position around the optical current sensor in Figure 2.

The optical outputs of both voltage and current sensors (i.e., the prisms of Figure 1 and Figure 2 respectively), hold the data of voltage/current amplitudes, in an optical-based form. The resulting light-based data must be in turn processed to offer more ''readable'' information. For this purpose, exists the optical modulate M410B from Micatu, as depicted in Figure 3 [25].

The modulator of Figure 3 consists of four modular bays, where in each a fiber optic cable (i.e., representing the fiber output for each of the prisms) with its corresponding terminal can be inserted. With that being said, the M410B represents thus the brain of the RG235 sensor, having a numerous ''plug and play'' options for different sensor modules. Such a platform encloses analog/digital outputs, allowing it thus to interface with various industrial and

substation automation systems. Successively, it is provided by the platform shown in Figure 3 some Low Energy Analog (LEA) outputs from 0 VAC to 10 VAC that can be used to observe the reflected output voltage/current after their internal transformation by the modulator itself. All readings of the voltage/current quantities processed by the optical modulator can be accessed by means of a peer-to-peer communication (using a serial to bus cable) with a computer, or by using its embedded local area network adapter, thus allowing it for remote control sessions [25]. Regardless of the communication mediums between the M410B and the computer, two software (windows based) exist, that are able to debug the modulator, listed as follows:

a. Micatu's graphical user interface [20]: representing a graphical visualization tool, where the voltage/current values can be read from each bay. Also, such software allows the configuration of the modulator, such as setting its internet protocol address, defining the input/output ratio for calculating the voltages/currents, setting the operational frequency, and other settings. What differs this method from the succeeding other, is that it requires no shell commanding, in which the user can simply configure the M410B by clicking on the desired setting/configuration. From another part, this method lacks instantaneous readings, where it only displays readings as snapshots recorded every 10 minutes
b. PuTTY [26]: used as a file transfer protocol where it can connect to the M410B (i.e., remote machine) using secure shell protocol for send/receive data processes from a remote server. Where the operating system of the M410B is Linux, a certain set of commands can be used in PuTTY to write/read data to/from the M410B: there are two submenus when starting a session with the modulator, the first corresponds to a general set of commands that can be addressed using the label ''factory''. The other is more specific and can be addressed using the label ''dnpcli''. Despite that this technique requires special commands' syntaxes, but it offers on the other hand, instantaneous readings for current/voltage values, as well as an overall status of the M410B. For example, instead of just graphically reading the voltage's value on bay1 in the graphical user interface, corresponding to the voltage level inputted to the modulator's first channel, the command ''factory getdata va'' must be typed in the logged shell session in the PuTTY interface.

III. EXPERIMENTAL SETUP

The commissioning procedures of the RG235 were held in the high voltage laboratory at the Helmut-Schmidt-Universität/Universität der Bundeswehr [27]. The series of tests conducted over the RG235 are composed of voltage and current measurements experimentations, separately. According to the RG235's design, Micatu [20] insists that the sensor should be projected to voltage and current simultaneously, in order for it to produce accurate measurements' outputs. Additionally, during the first week of the initial installation of the RG235, the latent will be in a self-learning-phase, such that according to the machine intelligence which is embedded in the M410B, it will constantly during that phase, calibrate the measuring resolution. Despite these two facts about the RG235, they were not actually taken into consideration when commissioning the sensor in the high voltage laboratory. It is otherwise intended to notice the error between the measurements' differences, the output curves behavior, the faults that might incorporate with the sensor's functioning. This strategy was perceived as having forced irregular conditions over the sensor, considered as an accelerated stress-test, constituting an emulative way to predict the sensor's behavior under faulty TL scenarios (e.g., load cutoff, etc.). With the stated test benchmark, it can be predictively acknowledged the sensor's behavior in cases where for example the TL is disconnected due to a force majeure, or when the load is faultily islanded.

TABLE 1. The testing transformer's electrical characteristics.

Characteristics	For each transformer	For the entire set of sub-transformers
Nominal voltage	2x0.22/100/0,22 kV	2x0,22/200 kV
Rated current	2x11.4/0.05/22.7 A	2x22.7/0.05 A
Rated power	5 kVA	10 kVA
Frequency of operation	50 Hz	50 Hz
Primary voltage	220 V	440 V
Secondary voltage	100 kV	200 kV

A. VOLTAGE MEASUREMENT EXPERIMENTATION

1) CONCEPT

In order for the RG235 to be tested for voltage measurements (having its operational voltage measurements range from 0 V to 35 kV), it must be supplied with a controllable voltage supply. The supply shall ideally be an auto-transformer, having its implementation taking into consideration all the precautions related to safe high-voltage based experimentations (i.e., earthing, arcing distance, interference, etc.). For this purpose, the RG235 has been fed by a test transformer (with a cascaded circuitry, composed of two sub-transformers) that has the electrical characteristics as encapsulated in Table 1 [28].

The feeding transformer with the electrical characteristics shown in Table 1 is operated and controlled distantly by means of a digital measuring instrument from Haefly Trench (DMI551) [29]. For personnel and equipment security purposes, the output of the high voltage transformer is grounded through three normally closed switches, inside the high voltage laboratory, consisting as follows:

- A pneumatic switch, controlled by the DMI551, that opens the circuit between the ground and the transformer's output, when manually set by the operator
- An earth rod, that only opens the circuit between the ground and the transformer's output, when placed on a

specific node of conducting material in the high voltage laboratory
- A normally closed switch by the Faraday's cage door inside the high voltage laboratory, that only opens the circuit between the ground and the transformer's output when the door is closed (for personnel safety)

These mentioned three normally closed switches are placed successively after a 10 $M\Omega$, 60 W resistor, used as a current limiter, before the output capacitor of 100 pF, 100 kV. The output capacitor is in turns connected through a two-part capacitive divider, and has a self-discharge mechanism. The RG235 is to be placed in the middle way between the current limiting resistor, and the output capacitor, with its earth terminal connected to the earth of the entire circuit. An additional North Star, High Voltage Probe [30], is added to the circuit as a reference voltage sensor. This in turns would allow a further graphical investigation of each sensor's output voltage curve, in response to the input set of voltages originated from the DMI551.

2) MONTAGE REALIZATION

The circuit concept description, can be graphically represented as a real circuit implementation as in Figure 4: the needed equipment (e.g., earth connection, etc.) for the circuit's realization can be installed by drag-and-drop inside the high voltage laboratory. This fact also applies for the connection lines (i.e., considered as the TL in the case of a real electrical grid). Additionally, a DEWETRON standalone oscilloscope, monitored by Oxygen software [31] is inserted in the circuitry, to visualize the output curves. The DC supply in Figure 4 is used to power up the M410B optical modulator, where the DC/AC supply, utilizes a recharged battery in order to produce an AC output voltage to be fed into the DEWETRON: it is used in order to remove any other AC signals inside the Faraday's cage, beside the output of the HV transformer (as a preventive way to mitigate any possible interference). Both of the voltage sensors' (i.e., HV probe and RG235) outputs are connected to the DEWETRON's input channels in order to have a graphical representation of both voltage curves within the same time-voltage plane.

B. CURRENT MEASUREMENT EXPERIMENTATION

1) CONCEPT

Although the RG235 is designed to be simultaneously supplied with both voltage and current (i.e., the circuitry of Figure 4 is supposedly enough to produce voltage/current output waveforms) but in this experimentation, the current was separately forced to flow across the RG235. As previously mentioned in this manuscript, this was due for experimentation purposes only, and to have an overview of the sensor's behavior when only subjected to voltage or current. By means of the Yokogawa 2558A current source, which has its electrical characteristics encapsulated in Table 2 [32], the RG235 was continuously subjected to different current values from 0 A to 60 A of 50 Hz frequency.

TABLE 2. The yokogawa 2558A electrical characteristics [32].

Criteria	For each transformer	For the entire set of sub-transformers
AC voltage	Output range of the specified accuracy	1.00 mV to 1200.0 mV
	Accuracy (50/60 Hz)	± 400 ppm
	Frequency of the specified accuracy	40 to 1000 Hz
AC current	Output range of the specified accuracy	1.00 mA to 60.00 A
	Accuracy (50/60 Hz)	± 500 ppm
	Frequency of the specified accuracy	40 to 1000 Hz
Max output		Approximately 36 VA

As was the case with the voltage measurement experimentation, a reference current measuring device SE-CUR-CLAMP-150-DC [33], was also added to this experimentation, in order to have both actual/reference current output curves.

2) MONTAGE REALIZATION

By using the same environment as of the voltage measurement, inside the high voltage laboratory (having the HV transformer turned off) the outputs of the Yokogawa 2558A can be attached to the rod passing through the RG235, as shown in Figure 5(a).

The reference current sensor is to be as well clamped around the same current carrying rod (i.e., representing the TL) across the RG235. The output fiber optical cable from the RG235 is to be connected to the optical modulator M410B (as was the case for the voltage measurement experiment), where its LEA output in addition to the output of SE-CUR-CLAMP-150-DC are to be connected to the DEWETRON. The entire current measurement circuitry is shown in Figure 5.

IV. RESULTS, OBSERVATIONS, AND FUTURE WORK

Prior to starting the voltage/current measurements' processes (i.e., setting different V/I referenced values then observing the RG235's output), on the first hand, the nominal frequency of the M410B must be changed to 50 Hz. This is a must, since it comes with a factory setting of a 60 Hz frequency, that should be changed in order for the M410B to be able to accommodate the electrical grid's frequency inside the Helmut-Schmidt-Universität/Universität der Bundeswehr. On the second hand, the internet protocol of the M410B must be also changed to a static value that lies within an accessible local area network (this is to ensure a remote access connection of the M410B, preferably from the outside of the high voltage laboratory, for a more secured personnel safety). In order to accomplish the mentioned tasks, a peer-to-peer connection is needed between the M410B and a host computer (i.e., between the local area network adapter of a computer, and the RG45 socket of the

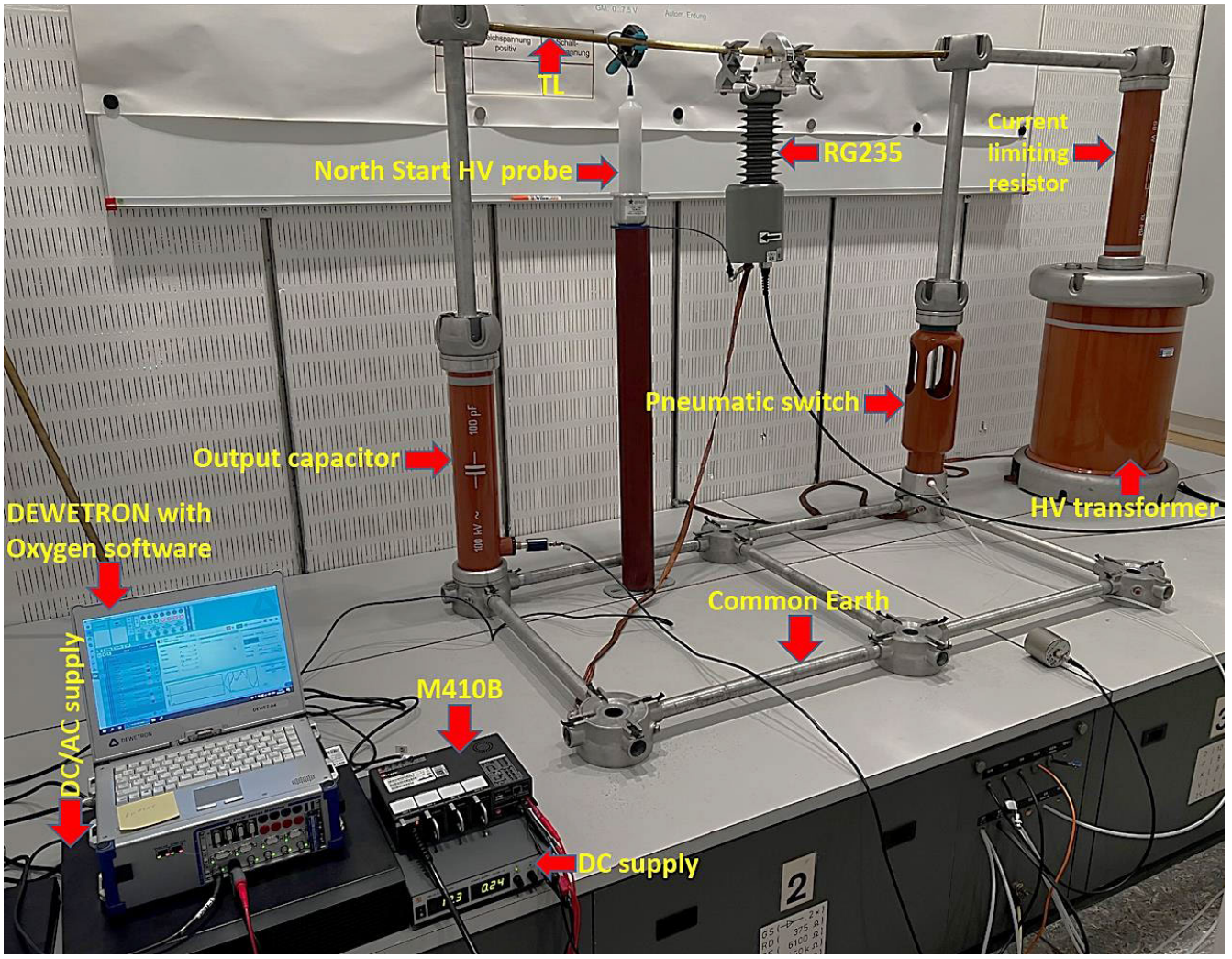

FIGURE 4. The RG235 high voltage test setup.

M410B, using a full-channel local area network cable). Once connected, firstly the network adapter of the host computer is to be statically set according to the factory domain address of the M410B. Then, by means of PuTTY, the host computer can access the M410B using its factory set internet protocol with the default username/password credentials. The textual interface presented by the PuTTY allows the command input lines (i.e., Linux-based of a special syntax) to be addressed to the M410B. Accordingly, Table 3 presents the command lines for changing the frequency as well as the internet protocol address for the M410B.

TABLE 3. Initial configuration of the m410B.

Configuration	Command syntax
Changing the M410B nominal frequency	1. dnpcli config nominallinefrequency 50 2. dnpcli config write 3. reboot
Changing the M410B internet protocol address	1. Config_network static 2. <enter the desired internet protocol address> 3. reboot

A. VOLTAGE MEASUREMENT OUTCOMES

The first step in this task is to open the previously stated normally closed (to earth) switches, consisting of the pneumatic, open-door, and earth switches conventionally (i.e., closing the high voltage laboratory lab's door, opening the pneumatic switch, and placing the earth's stick onto its designed location). Then, the Haefely Trench's controlled root mean square output voltages are manipulated from 1.413 kV to 20.464 kV (the maximum supported voltage by the North Pole, High Voltage Pole was taken into consideration consequently). Through different voltage values between the stated limits, the RG235's measured voltage values were time-lapse recorded as revealed in Table 4. That table also shows the percentage of error, as calculated in (3), between the actual

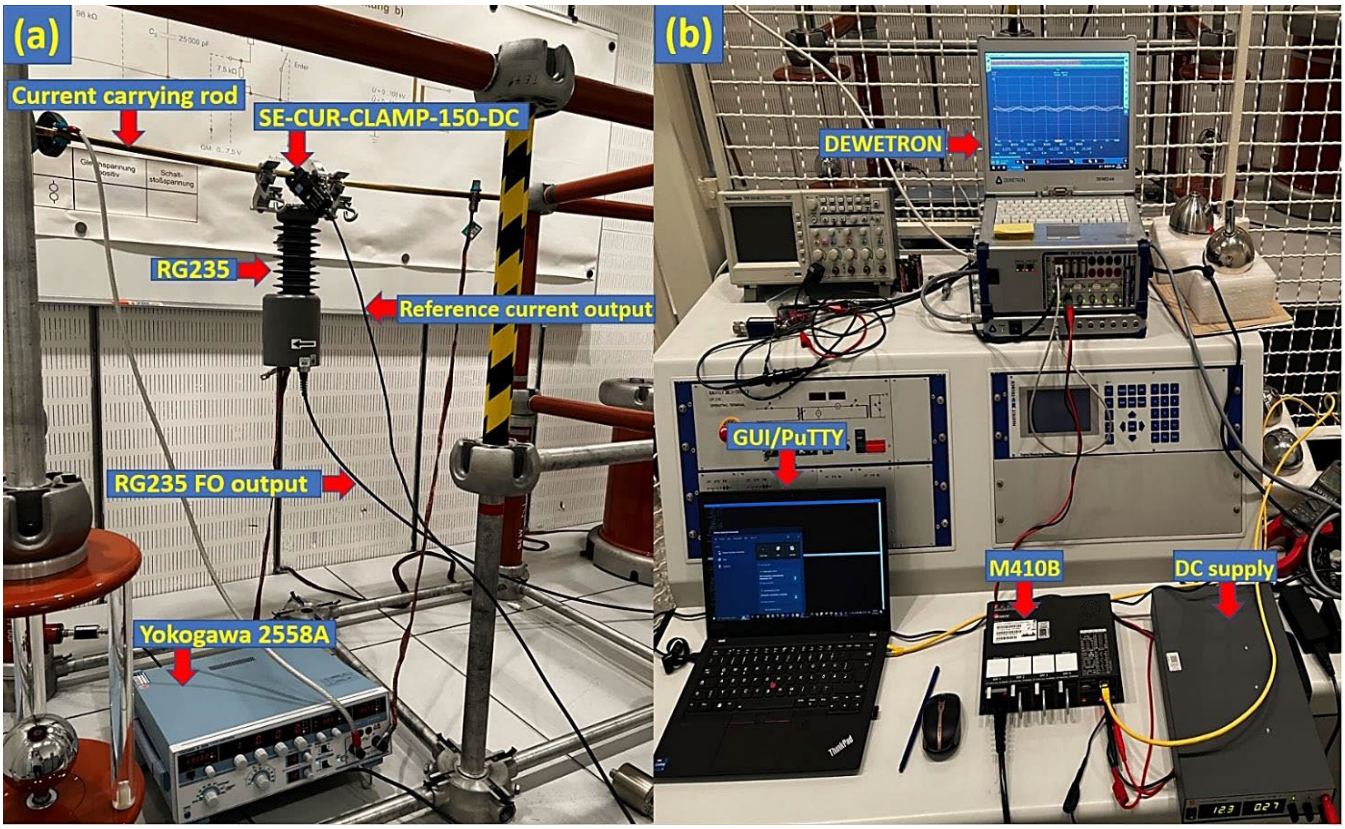

FIGURE 5. The RG235 current test setup, (a) circuitry, (b) output assembly.

TABLE 4. Tabulated voltage measurement data.

Reference root mean square voltage [kV]	Actual root mean square voltage [kV]	Percentage of difference error [%]
1.413	1.286	9.00
2.385	2.532	6.17
3.142	3.351	6.66
4.438	4.006	9.75
5.730	5.253	8.32
6.687	6.174	7.70
7.740	7.124	7.97
8.990	8.319	7.47
9.755	9.813	0.39
10.710	10.019	6.46
11.855	11.115	6.23
12.687	11.958	5.74
13.857	13.147	5.12
14.603	14.022	3.98
15.602	15.078	3.36
16.450	15.975	2.89
17.294	16.929	2.12
18.587	18.500	0.47
19.879	20.194	1.59
20.464	21.039	2.82

measured voltages (i.e., the RG235 outputs) and the reference values (i.e., the North Pole HV Probe outputs).

$$\%Error = \frac{|(Reference\ value - measured\ value)|}{Reference\ value} \times 100 \tag{3}$$

By having the LEA of the RG235 (which is outputted from the M410B) and the analog output of the North Pole HV probe, connected to the first rack, first and second channels (AI 1/1, AI 1/2) of the DEWETRON respectively, the resulting voltage measurements of Table 4, can be visualized as represented in Figure 6. In all measurements' visualizations, it was taken into consideration each of the RG235 as well as the North Pole HV probe input/output voltage conversion. For example, the term ''oratio'' in the RG235 settings, refers to the input/output value, which accordingly the sensor outputs the value for the correspondent LEA. Moreover, the setting of ''oratio'' of the RG235 can be manually adjusted by the command syntax ''factory oratio va 1400'': such a command line outputs a LEA representing the input voltage (on Bay1) divided by 1400 (i.e., for each 1.4 kV the LEA output is 1 V). With a similar characteristic existing also for the North Pole HV probe, the DEWETRON's oscilloscope settings can be well calibrated to have a standard output. Amongst different values in Table 4, the graphical representation of Figure 6, takes into consideration the last voltage pair (i.e., (20.464 kV; 21.039 kV)). It is also to be declared that, the voltage measurements by the RG235 can be monitored from the Micatu graphical user interface, as well as the PuTTY (i.e., the syntax ''factory getdata va'' for example outputs the measured voltage on Bay1).

B. CURRENT MEASUREMENT OUTCOMES

The montage of Figure 5(a) allows a dynamic current flow across the RG235. By means of the output current rotary

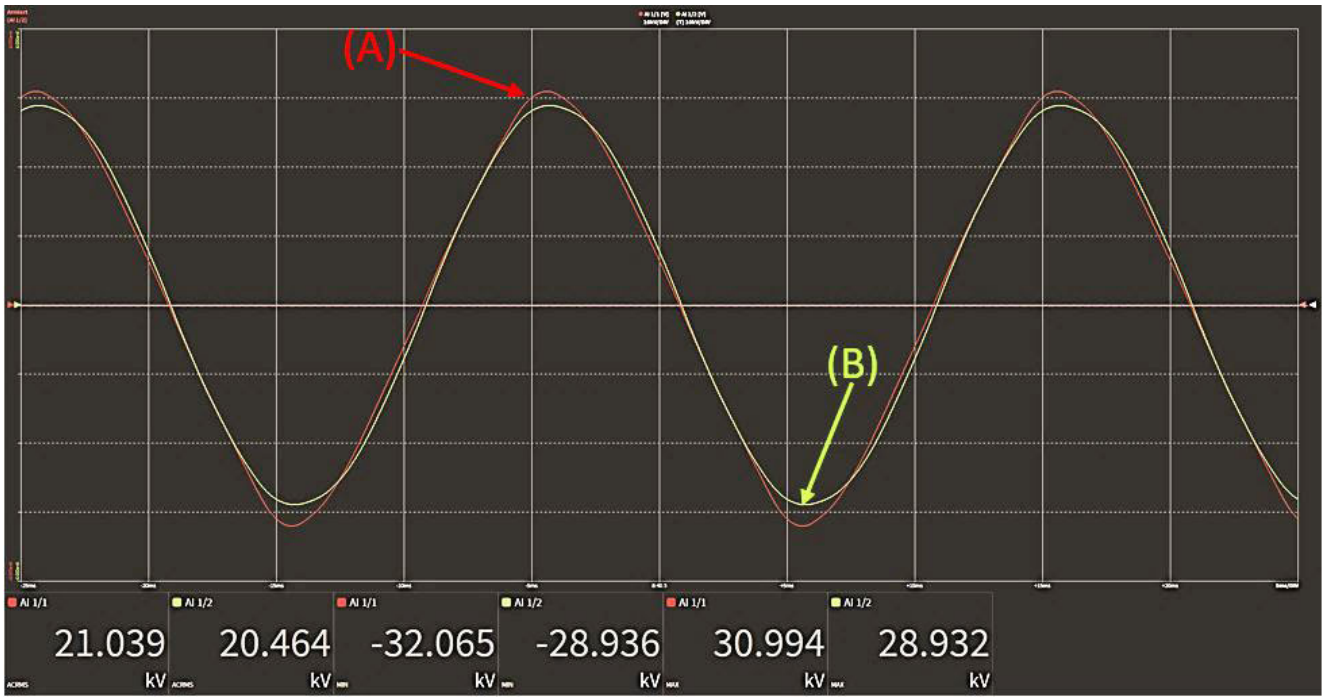

FIGURE 6. The DEWETRON output voltage curves, (A) RG235, (B) north pole high voltage probe.

TABLE 5. Tabulated current measurement data.

Reference root mean square current [A]	Actual root mean square current [A]	Percentage of difference error [%]
10	11.81	18.1
20	23.05	15.25
30	34.74	15.8
40	46.29	15.725
50	58.49	16.98
60	70.082	16.803

switch of the Yokogawa 2558A, different current values from 10 A to 60 A were injected in the current carrying conductor (i.e., representing the TL in an electric grid), which is passing through the air gap of the current concentrator of the RG235. As presented in Table 5, the RG235's measured current values were time-lapse recorded, where it is also shown the percentage of error, calculated using (3), between the actual measured currents (i.e., the RG235 outputs) and the reference values (i.e., the SE-CUR-CLAMP-150-DC outputs).

As is the case for the voltage measurement principle of the RG235, an ''oratio'' also exists for the current, such that the values of Table 5 are recorded when the ''oratio'' was manually set to 60, using the command syntax: ''factory oratio ia 60''. Such a command line, in turns, outputs a LEA representing the input current (on Bay1) divided by 60 (i.e., for each 60 A the LEA output is 1 V). In order to not neglect the powerful monitoring facility provided by the PuTTY in regards to voltage as well as current measurements by the

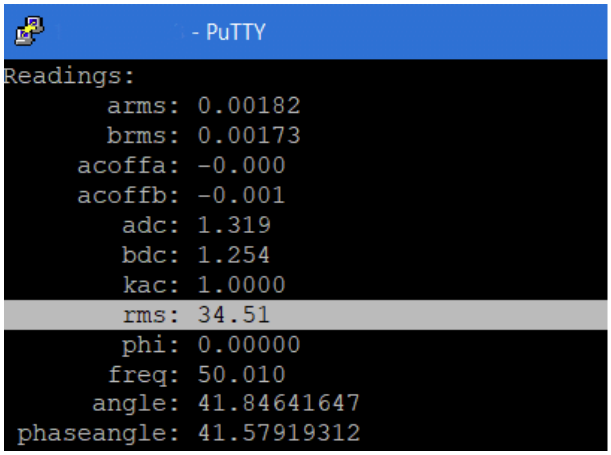

FIGURE 7. A PuTTY-based current measurement reading.

RG235, and as was the case for the voltage measurements, it is possible to observe the sensed current values, textually. For instance, the command ''factory getdata ia'' fetches out the sensed current value on Bay1 of the M410B, as can be seen in Figure 7, when the reference set current was of 30 A. It is to be noted that the RG235, according to Figure 7, can as well measure the frequency (50.010 Hz) and the phase angle (41.579). This ability to measure other than V/I quantities is perceived as an added value in real world applications, yielding eventually in a better monitoring approach for TL.

Concerning the current curves outputs, and as was the case also with the voltage measurements outcomes, the analog output of the SE-CUR-CLAMP-150-DC as well as the

LEA of the M410B (i.e., representing the modulated optical input from the RG235 under current tests) are to be connected to the first rack, first and second channels of the DEWETRON respectively. By taking into consideration the input/output current conversion ratios of both the RG235 and the SE-CUR-CLAMP-150-DC, the oscilloscope settings of the DEWETRON can accordingly be adjusted, thus yielding in a standardized and a calibrated output current curves. Amongst different values in Table 5, the graphical representation of Figure 8 corresponds to the current pair of (60 A; 70.082 A).

C. DISCUSSION

The presented tabulated data in both Tables (4-5) gives a clear indication over the necessity of the 7-day self-calibration period: for voltage measurements exists an averaged error deviation of 5.21% where for the current measurements the average error is of 16.414%. This can be as well justified after the visualization of Figure 6 and Figure 8: not only the voltage/current curves show a deviation in the outputted AC max values, but it can be also concluded that the AC voltage/current of the referenced/measured quantities have a slight phase shift (i.e., the resultant AC curves do not zero-cross the time axis instantaneously). It is noticed that during current tests only (i.e., with the absence of any applied voltage), the RG235 declares a ''PU'' fault, where it gets unable to phase lock on the voltage signal. During other V/I measurements, it was witnessed through different experimentations that sometimes the LEA curves produced by the M410B, get severely distorted in both phase angle and AC max values, with respect to the reference values. Such consequences are mainly due to the absence of simultaneous voltage and current across the RG235. Moreover, and as stated by Micatu, the calculated average error deviations for voltage and current measurements are supposed to be flattened initially after a ''learning'' period, during which the M410B can better calibrate its output measurements' accuracy. In other terms, the difference in the sinusoidal output curves of both Figure 6 and Figure 8 is due to temporary false data interpretation of the light's polarization rotation. This can be justified with the fact that the RG235 during the first commissioning was still ''learning'' how to accurately proceed with LEA according to the sensed input.

Aside than the stated errors in measurement (although justified), the RG235 showed an excellence reliability, where its fiber optical output cable reduces the risk of any possible interference: for example, the reference North Pole High Voltage probe did not support such a feature, and consequently a remote access to the DEWETRON was needed for a better personnel safety in case of any possible interference. Additionally, the internet protocol addressing supported by the RG235 enables a dynamic remote access: under the theme of ''smart grids'', by means of the M410B, an electric grid can become actually ''ping-able'', such that the installed RG235 over a TL's portion makes the latent network addressable. Hence, by means of the added remote monitoring capability to the grid, predictive mathematical models can be more easily implemented, thus better maintaining the grid preventively.

In relation to the DNeD project, the most important criteria regarding the RG235 commissioning is its feasibility study for future implementation inside the DNeD's drone: the optical based process measurements (i.e., Pockels' effect for voltage and Faraday's magneto-optical for current) offer a reliable and a safe measurement option, but it requires a certain insulation level that can be reflected with the bulky overall design of the RG235. The following key points summarize why the RG235 cannot be directly implemented in the drone of the DNeD project:

- Heavy weight/bulky design: the RG235 sensor and as can be seen from the Figures (4-5), requires a definite space of installation, and is too heavy to be carried up with a drone
- ''Relative'' contactless V/I measurements: In order for the RG235 to sense the voltage of the TL, it must be actually in contact with it (the clamping connectors constitute the physical touch with the TL, thus representing the resulting electric field transfer medium to the Pockels' sensor). Therefore, it cannot be incorporated in a drone-based TL remote monitoring application, since the supposed sensor (i.e., inside the black box of the DNeD's drone) must be able to sense the voltage/current actively while being away from the TL. The same fact also applies for the current sensing, since the RG235 requires its current concentrator to be clamped all around the TL, and this is also not applicable for any drone-based TL monitoring processes
- Auxiliary equipment: the RG235 alone is incapable of producing any significant (i.e., human-readable) measurements, as it needs to be connected to the M410B, in order for the latent to modulate the incoming optical signals into processable data. This fact composes an obstacle for the RG235 to be incorporated in the DNeD's project drone, since it is impractical to have a fiber optical connector, a fiber optical modulator, and a DC supply for the modulator, inside of the drone's black box. The needed sequential block connections for the optical V/I measurements realization make it hard for such design to be fit in a drone-based application, due to size constraints mainly. Furtherly, and by taking into consideration the intended workflow of the DNeD project (i.e., the black box is to be thrown from the TL, all the way to the ground) it can be declared that a fiber optics modulator is too fragile to be installed in such a box, as it would certainly be deteriorated after the fall down from the TL.

D. VIBRATION TEST

As intended to employ the RG235 in a drone, it is crucial to test its behavior under vibrating conditions. Since drones generally involve multiple propellers/rotors, some significant vibrations can be generated during the flight.

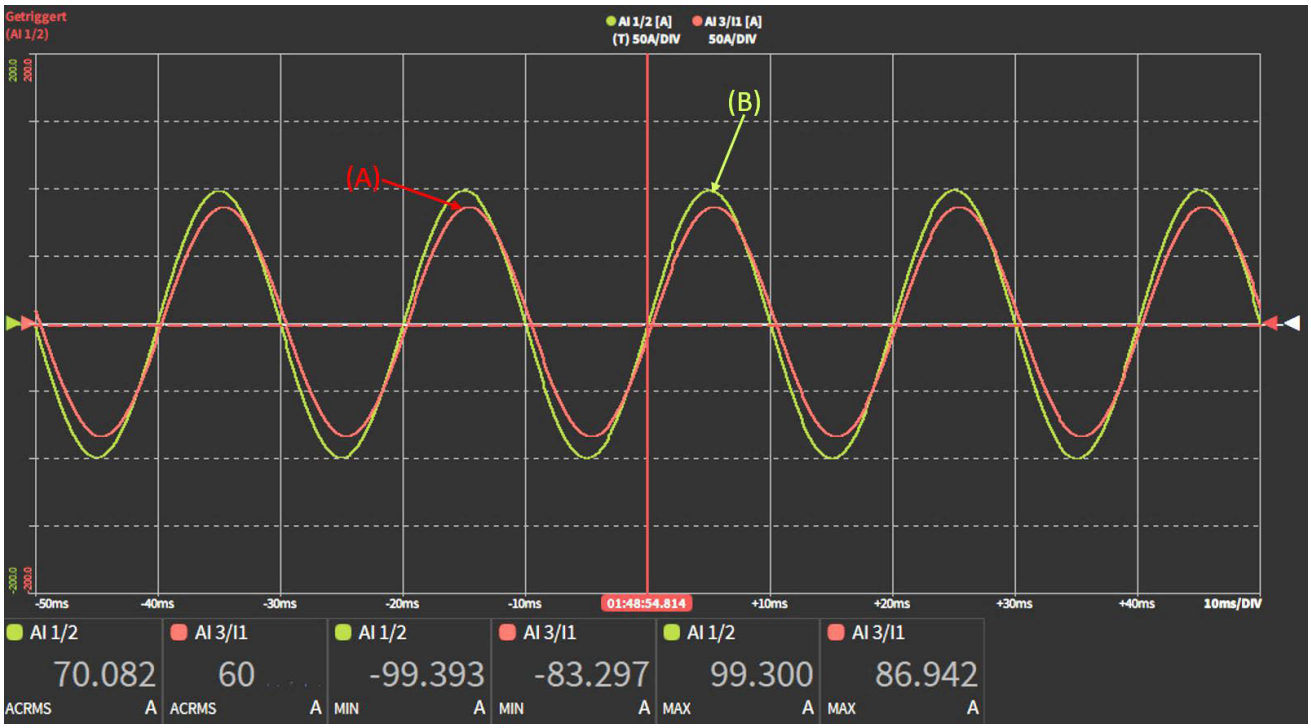

FIGURE 8. The DEWETRON output current curves, (A) SE-CUR-CLAMP-150-DC, (B) RG235.

This is mainly due to the rapid rotation of the propellers, to the drone's movements during acceleration/deceleration, and changes in directions. Therefore, such induced vibrations can impact both of performance as well as the reliability of the RG235 when actually employed in a real drone application. For instance, continuous vibrations can create an excessive mechanical stress, which can be reflected as an accelerated physical damage to the RG235's structural elements. Additionally, under vibrations, different signals can be deteriorated with a possible total loss in the communication links. For these stated reasons, and in order to accurately acknowledge whether the sensor can perform good measurements under vibrating conditions, an artificial vibration test was conducted on the RG235, under the same experimental setup of Figure 4 and Figure 5.

It is to be clarified that, the RG235 is being used in this part of the experiment after a completed 7-day learning period (i.e., during which the RG235 was continuously subjected to current and voltage).

With this experimental approach, the residual error in Table 4 and Table 5 can be concretely checked, simultaneously while investigating the RG235's V/I readings under vibrations. This test specifications are listed as below, with the final V/I measurements listed in Table 6:

1. Currents across the RG235 are ranged from 10 A to 60 A, as was the case during the initial current measurement's experimentation
2. Voltages supplied to the RG235 are of randomly increasing values from 0 kV to 20 kV
3. The vibration test was conducted for 20 minutes (as assumed to be the duration of the drone's flight around the TL), with a low-frequency vibration of 5 Hz (300 cycles per minute). A controller-based vibration test system is applied to the RG235's encapsulant.

TABLE 6. Tabulated voltage and current measurements final data.

VOLTAGE MEASUREMENTS				
Ref. RMS voltage [kV]	Measured RMS voltage [kV] (no vibrations)	Measured RMS voltage [kV] (under vibrations)	Error [%] (no vibrations)	Error [%] (under vibrations)
1.542	1.530	1.500	0.77	2.72
2.573	2.563	2.646	0.39	2.84
3.762	3.719	3.851	1.14	2.37
5.199	5.228	5.026	0.56	3.33
6.385	6.469	6.553	1.32	2.63
7.946	7.969	8.161	0.29	2.71
8.641	8.692	8.414	0.59	2.63
9.875	10.035	10.129	1.62	2.57
10.318	10.241	10.596	0.75	2.69
12.847	13.049	12.516	1.57	2.58
14.726	14.920	14.965	1.32	1.62
16.203	16.273	16.058	0.43	0.89
18.912	19.120	18.611	1.10	1.59
19.624	19.996	19.419	1.90	1.04
CURRENT MEASUREMENTS				
Ref. RMS current [A]	Measured RMS current [A] (no vibrations)	Measured RMS current [A] (under vibrations)	Error [%] (no vibrations)	Error [%] (under vibrations)
10	10.11	9.71	0.89	2.90
20	20.31	20.77	1.55	3.84
30	30.62	31.01	2.07	3.37
40	40.46	41.31	1.14	3.28
50	49.66	52.12	0.68	4.24
60	60.15	60.88	0.25	0.18

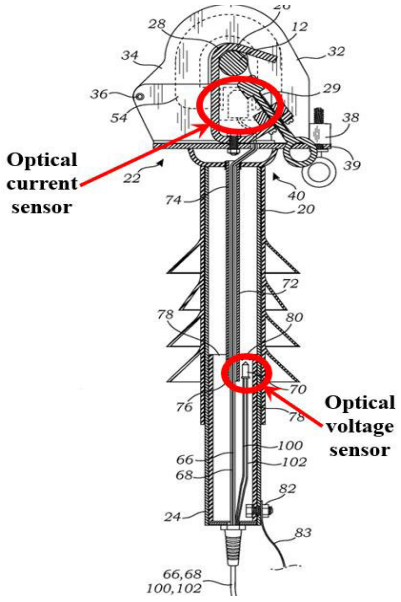

FIGURE 9. The RG235's internal V/I optical sensors [24].

FIGURE 10. The mechanical holders of the drone's black box [18].

It is evident, according to the data of Table 6, and as stated by Micatu, that the RG235 rectifies its error in V/I measurement after the needed 7-day learning period. For instance, during the learning period, the RG235 has shown an average percentage of error deviation between the reference voltage levels and the measured ones of 5.47%. This value got diminished to 0.989% after the completion of the learning period. The same fact also applies for the current measurements, where the percentage of the deviated error between reference and measured values fell from 16.443% to 1.097% before and after the learning period respectively. As concerning the effect of vibrations, it can be also stated that the RG235 is relatively immune to vibrating environments (in this case, the forced 5 Hz applied vibrations).

E. FUTURE WORK

Following the laboratory investigation of the RG235, it can be stated that the sensor cannot be directly employed in the DNeD project, despite the numerous advantages that it provides. Therefore, in order to grant the advantages presented by the sensor, thus sensing V/I optically (i.e., no electrons flow, no saturation, safe performance, etc.) a disassembly of the sensor's encapsulant is suggested as a future work. The V/I prisms (i.e., the Pockels based voltage sensor, and the Faraday's magneto-optical based current sensor) are to be removed from the cycloaliphatic epoxy body of RG235 and be placed inside the DNeD project drone's black box. The corresponding advantageous point is that both current and voltage sensors are too small in size, and can be easily installed in the black box, that is intended to be used as an area for the sensor's installation. The referred optical sensors are circulated in red in Figure 9.

In order to modulate the output coming signals through the optical cords of the V/I sensors of Figure 9, a singular input channel (i.e., Bay1) amongst the four presented in the M410B can be re-structured to carry the light-based information, and be placed near the optical prisms inside the drone's black box. However, the suggested RG235 modified design still needs a closed looping around the TL, in order for the optical current sensor to be able to captivate the resulting optical image of the magnetic field, which is resulting from the flow of current. For this purpose, the mechanical clamp holders of the DNeD drone's black box are suggested to be a part of the current sensor, since the material of ferrite iron for example, can be "stuffed in" the plastic material that is composing the box's mechanical holders, highlighted in red, as revealed in Figure 10.

Accordingly, the Micatu's current concentrator of its original design (i.e., label "54" in Figure 9), can be embedded inside the mechanical holders shown in Figure 10. Moreover, the RG235's reshaping, for it to be fit into the box of Figure 10, would neglect any need for any connection to ground. With that being said, the intrinsic insulation coordination, which fulfills the electrical safety standards, including arcing and creepage distances for example, will not be needed for the black box (i.e., there would not be for example two conductive parts at different electric potentials inside the black box).

As for the voltage measurements, a small conductive rod can be forced upwards (i.e., to the outside of the black box) by means of an embedded DC motor, constituting hence an electric field transfer medium to a small computerized system (inside the black box, which also controls the DC motor) for further analysis of the obtained V/I measurements' data. The final output V/I measurements can be electrostatically saved by means of an analog data storage device. For instance, a "memristor" [34] can save analog voltage values, by remembering its resistance based on the amount of charge passing through it previously. Even after the feeding power

is turned off, memristors can remember their last resistance value, hence composing a potential solution for the DNeD's analog data storage (i.e., different voltage levels are stored as different resistance states). Such recorded ''values'' can be stored by the controlling computerized system in the black box, for later analysis, through different possible communication protocols. The entire setup inside the black box can be powered up by means of a small powered Lithium-Ion battery, since this circuit would be only turned on temporarily (i.e., for few minutes, under each actual test procedure). Another crucial point to be taken into consideration, is the fact that the box of Figure 10 is intended to fall from height (i.e., all the way from the TL to the ground) in order for an operator to take it for future data extraction and analysis. For this purpose, especially with the reconfigured assembly of the RG235, the referred box must have a shock-resistant mechanical enclosure in it, preferably with a shock absorbing material, such as foam or elastomers [35].

V. CONCLUSION

Smart grids represent a potential solution towards a greener power production and a carbonless future. Concerning the different methods through which an intelligence can be added to a conventional electric grid, the installation of smart sensors (e.g., the RG235 sensor) is an effective scheme allowing a remote TL's monitoring option. The RG235 investigated in this paper, adds a network-addressable ''ping'' function over a TL, allowing hence remote monitoring ability and a precise TL's status reading, with an enhanced safety for both personnel as well as the equipment. Thus, preventive maintenance strategies can be better applied on electric grids, reducing the probabilities of blackouts and allowing an enhanced TL's performance optimization. In order to employ the investigated ''all-optical'' RG235 sensor in the exposed DNeD project (i.e., to install the sensor inside the drone's black box), this paper has clarified its main re-structuring key points, mainly related to size restrictions where the Pockels/Faraday optical sensors are to be detached from the RG235's Cycloaliphatic Epoxy body, to be directly installed inside the drone's black box (assuming the latent is to be as well reconfigured with a shock absorbing structural design). The modulated data outcomes are to be furtherly processed by a small, battery-powered computerized system (e.g., Arduino, Raspberry Pi, etc.). After the laboratory tests conducted by this paper, it is encouraged to furtherly test and report the actual suggested re-structuring of the RG235, and to tabulate the measurements observation under real TL monitoring applications.

REFERENCES

[1] W.-T. Lin, G. Chen, and H. Li, ''Carbon-aware load balance control of data centers with renewable generations,'' *IEEE Trans. Cloud Comput.*, vol. 11, no. 2, pp. 1111–1121, Apr./Jun. 2022, doi: 10.1109/TCC.2022.3150391.

[2] T. R. Chaves, M. A. I. Martins, K. A. Martins, and A. F. Macedo, ''Development of an automated distribution grid with the application of new technologies,'' *IEEE Access*, vol. 10, pp. 9431–9445, 2022, doi: 10.1109/ACCESS.2022.3142683.

[3] I. Akhtar, S. Kirmani, and M. Jameel, ''Reliability assessment of power system considering the impact of renewable energy sources integration into grid with advanced intelligent strategies,'' *IEEE Access*, vol. 9, pp. 32485–32497, 2021, doi: 10.1109/ACCESS.2021.3060892.

[4] C.-Y. Chen, Y. Zhou, Y. Wang, L. Ding, and T. Huang, ''Vulnerable line identification of cascading failure in power grid based on new electrical betweenness,'' *IEEE Trans. Circuits Syst. II, Exp. Briefs*, vol. 70, no. 2, pp. 665–669, Feb. 2023, doi: 10.1109/TCSII.2022.3213552.

[5] Z. Wang, ''A novel evaluation method of transmission grid performance in power spot market,'' *IEEE Access*, vol. 7, pp. 181178–181183, 2019, doi: 10.1109/ACCESS.2019.2953009.

[6] X. Wu, H. Xiong, S. Li, S. Gan, C. Hou, and Z. Ding, ''Improved light robust optimization strategy for virtual power plant operations with fluctuating demand,'' *IEEE Access*, vol. 11, pp. 53195–53206, 2023, doi: 10.1109/ACCESS.2023.3280057.

[7] Y. Li, P.-H. Cui, J.-Q. Wang, and Q. Chang, ''Energy-saving control in multistage production systems using a state-based method,'' *IEEE Trans. Autom. Sci. Eng.*, vol. 19, no. 4, pp. 3324–3337, Oct. 2022, doi: 10.1109/TASE.2021.3118226.

[8] X. Liu, X. Li, J. Tian, G. Yang, H. Wu, R. Ha, and P. Wang, ''Low-carbon economic dispatch of integrated electricity-gas energy system considering carbon capture, utilization and storage,'' *IEEE Access*, vol. 11, pp. 25077–25089, 2023, doi: 10.1109/ACCESS.2023.3255508.

[9] S. Gangatharan, M. Rengasamy, R. M. Elavarasan, N. Das, E. Hossain, and V. M. Sundaram, ''A novel battery supported energy management system for the effective handling of feeble power in hybrid microgrid environment,'' *IEEE Access*, vol. 8, pp. 217391–217415, 2020, doi: 10.1109/ACCESS.2020.3039403.

[10] A. Arabhosseini, ''Application of clean energies in agricultural greenhouses,'' in *Proc. 8th Int. Conf. Technol. Energy Manage. (ICTEM)*, Feb. 2023, pp. 1–5, doi: 10.1109/ICTEM56862.2023.10084219.

[11] C. Hu, W. Wang, Y. Cai, H. Xue, Y. Kang, and Z. Cai, ''Communication scheduling strategy for the power distribution and consumption Internet of Things based on dynamic priority,'' in *Proc. 5th Int. Conf. Renew. Energy Power Eng. (REPE)*, Sep. 2022, pp. 50–55, doi: 10.1109/REPE55559.2022.9949518.

[12] Q. Zhang, Y. Gao, W. Mo, F. Han, and L. Zhang, ''Load forecasting considering demand response mechanism,'' in *Proc. Panda Forum Power Energy (PandaFPE)*, Apr. 2023, pp. 1172–1177, doi: 10.1109/PandaFPE57779.2023.10140881.

[13] D. Shinghal, A. Saxena, N. Saxena, K. Shinghal, R. Misra, and S. Saxena, ''Intelligent control and stability assessment of smart grid required for electric vehicles,'' in *Proc. Int. Conf. Adv. Comput., Commun. Mater. (ICACCM)*, Nov. 2022, pp. 1–4, doi: 10.1109/ICACCM56405.2022.10009516.

[14] Z. Liu, P. Li, B. Tian, J. Zhao, Y. Hu, H. Sun, X. Yin, Z. Wang, and M. Guo, ''Current and voltage measurement method based on magnetic and electric field sensors for smart grid applications,'' in *Proc. IEEE 4th Conf. Energy Internet Energy Syst. Integr. (EI2)*, Oct. 2020, pp. 2783–2786, doi: 10.1109/EI250167.2020.9346919.

[15] M. A. H. S. Midul, S. H. Pranta, A. S. I. Biddut, S. I. Siam, M. R. Hazari, and M. A. Mannan, ''Design and implementation of IoT-based smart energy meter to augment residential energy consumption,'' in *Proc. 3rd Int. Conf. Robot., Electr. Signal Process. Technol. (ICREST)*, Jan. 2023, pp. 106–110, doi: 10.1109/ICREST57604.2023.10070068.

[16] M. Pau, M. Mirz, J. Dinkelbach, P. Mckeever, F. Ponci, and A. Monti, ''A service oriented architecture for the digitalization and automation of distribution grids,'' *IEEE Access*, vol. 10, pp. 37050–37063, 2022, doi: 10.1109/ACCESS.2022.3164393.

[17] M. H. Saeed, W. Fangzong, B. A. Kalwar, and S. Iqbal, ''A review on microgrids' challenges & perspectives,'' *IEEE Access*, vol. 9, pp. 166502–166517, 2021, doi: 10.1109/ACCESS.2021.3135083.

[18] Accessed: Sep. 5, 2023. [Online]. Available: https://www.hsu-hh.de/rt/forschung/dned

[19] Accessed: Sep. 5, 2023. [Online]. Available: https://www.micatu.com/measuring-with-light

[20] Accessed: Sep. 5, 2023. [Online]. Available: https://www.micatu.com/gridview-platform

[21] R. Weiss, A. Itzke, J. Reitenspieß, I. Hoffmann, and R. Weigel, ''A novel closed loop current sensor based on a circular array of magnetic field sensors,'' *IEEE Sensors J.*, vol. 19, no. 7, pp. 2517–2524, Apr. 2019, doi: 10.1109/JSEN.2018.2887302.

[22] A. Pradhan, M. Oshetski, S. Stelick, J. A. Sperrick, and W. Laratta, ''Optical pockels voltage sensor assembly device and methods of use thereof,'' U.S. Patent US 10 634 704 B2, Apr. 28, 2020. [Online]. Available: https://patents.google.com/patent/US10634704B2/en

[23] L. Yansong, J. Yaoyao, M. Lu, L. Jun, and Y. Qingqin, "Study on Faraday magneto-optical effect optical current transducer based on double closed-loop self-tuning system," in *Proc. 5th Int. Conf. Crit. Infrastructure (CRIS)*, Sep. 2010, pp. 1–5, doi: 10.1109/CRIS.2010.5617496.
[24] J. Y. Harlev, R. Veazey, T. Konetski, and L. Johnson, "Optical sensor assembly and method for measuring current in an electric power distribution system," European Patent EP 2 494 392 B1, Jun. 7, 2023. [Online]. Available: https://patents.google.com/patent/EP2494392B1/en?oq=EP2494392B1
[25] *Advanced Distribution Grid Monitoring System GridView M410B Voltage, Current, Temperature, & Vibration Sensing*. Accessed: Aug. 27, 2023. [Online]. Available: https://www.micatu.com/hubfs/Micatu%20%20M410B%20Brochure%202020_SM.pdf
[26] *PuTTY: A Free SSH and Telnet Client*. Accessed: Aug. 27, 2023. [Online]. Available: https://www.chiark.greenend.org.uk/~sgtatham/putty/latest.html
[27] *Helmut-Schmidt-Universität/Universität der Bundeswehr, High Voltage Laboratory*. Accessed: Aug. 23, 2023. [Online]. Available: https://www.hsu-hh.de/ees/en/dlab-2/high-voltage-laboratory-2
[28] Accessed: Sep. 5, 2023. [Online]. Available: https://ritz-international.com/produkte/transformatoren/
[29] Accessed: Sep. 5, 2023. [Online]. Available: https://www.pfiffner-group.com/products-solutions/details/2767
[30] Accessed: Sep. 5, 2023. [Online]. Available: https://www.highvoltageprobes.com/
[31] Accessed: Sep. 5, 2023. [Online]. Available: https://www.dewetron.com/de/messtechnik-produkte/oxygen-software/
[32] Accessed: Sep. 5, 2023. [Online]. Available: https://tmi.yokogawa.com/solutions/products/generators-sources/standard/2558a-ac-voltage-current-standard/
[33] Accessed: Sep. 5, 2023. [Online]. Available: https://ccc.dewetron.com/dl/5bd05307-d80c-4e42-b030-7f89d9c49a3c
[34] C. F. Bermudez-Marquez and J. M. Munoz-Pacheco, "Design guidelines for physical implementation of fractional-order integrators and its application in memristive systems," in *Mem-elements for Neuromorphic Circuits with Artificial Intelligence Applications*. New York, NY, USA: Academic, ch. 11, pp. 225–248, doi: 10.1016/B978-0-12-821184-7.00019-0.
[35] Z. Xu, G. Wang, J. Zhao, A. Zhang, G. Dong, and G. Zhao, "Anti-shrinkage, high-elastic, and strong thermoplastic polyester elastomer foams fabricated by microcellular foaming with CO_2 & N_2 as blowing agents," *J. CO2 Utilization*, vol. 62, Aug. 2022, Art. no. 102076, doi: 10.1016/j.jcou.2022.102076.

KHALED OSMANI received the M.Sc. degree in power electrical engineering from Lebanese International University, Lebanon, in 2016. He was an Engineering Laboratory Instructor with Lebanese International University, from 2017 to 2019. He was a Senior Design Engineer with "Organisme de Gestion et d'Exploitation de l'ex Radio Orient" (OGERO), Lebanon. After finishing his role as a Programmable Logic Controllers' Programmer for bio-gas plants in Germany, he is currently a Research Assistant with the Institute of Electrical Power Systems, Helmut Schmidt University/University of the Bundeswehr Hamburg, Hamburg, Germany. He has diverse scientific publications, where also he regularly reviews papers for different journals. His current Ph.D. research involves artificial intelligence based techniques for photovoltaic plants' performance optimization. His research interests include renewable energy supplies integration, applied mathematics, and smart grids.

MARC FLORIAN MEYER received the M.Sc. degree in electrical engineering from the Hamburg University of Technology, Hamburg, Germany, in 2016. He is currently a Research Assistant with the Institute of Electrical Power Systems, Helmut Schmidt University/University of the Bundeswehr Hamburg, Hamburg. His current research interests include the grid integration of renewable energies and power quality, which is pursued at Distributed Energy Laboratory (DLab).

FLORIAN GRUMM received the Dipl.-Ing. degree in electrical engineering from the Technical University of Berlin, Berlin, Germany, in 2012. From 2006 to 2012, he was a Development Assistant with opTricon GmbH. He is currently a Research Assistant with the Institute of Electrical Power Systems, Helmut Schmidt University/University of the Bundeswehr Hamburg, Hamburg, Germany. His research interests include protection of sources with limited short-circuit currents, change of protection of electrical distribution grids, optimizing aircraft power systems, and development of solid-state power controller, which are pursued at Distributed Energy Laboratory (DLab).

DETLEF SCHULZ (Senior Member, IEEE) received the Dipl.-Ing. degree in electrical engineering from the Technical University of Cottbus, Germany, in 1997, and the Dr.-Ing. and venia legendi degrees in electrical engineering from the Technical University of Berlin, Berlin, Germany, in 2002 and 2006, respectively. From 1997 to 1999, he was with ABB Industrial Automation, Cottbus, Germany. Since 2006, he has been a Full Professor and the Head of the Institute of Electrical Power Systems, Helmut Schmidt University/University of the Bundeswehr Hamburg, Hamburg, Germany. His research interests include electrical power systems and on-board electrical systems: grid integration of distributed generation, electro-mobility and hydrogen technologies, grid impedance measurement and grid protection, which are pursued at Distributed Energy Laboratory (DLab). He is a member of VDE ETG and IEEE PES and a Full Member of the Academy of Sciences and Humanities, Hamburg.